Rotational spectra of C_4N, C_6N, and the isotopic species of C_3N

M. C. McCarthy
Harvard-Smithsonian Center for Astrophysics, Cambridge, Massachusetts 02138
and Division of Engineering and Applied Sciences, Harvard University, Cambridge, Massachusetts 02138

G. W. Fuchs
I. Physikalisches Institut, Universität zu Köln, Zülpicher Straße 77, D-50937 Köln, Germany

J. Kucera
Harvard-Smithsonian Center for Astrophysics, Cambridge, Massachusetts 02138
and Division of Engineering and Applied Sciences, Harvard University, Cambridge, Massachusetts 02138

G. Winnewisser
I. Physikalisches Institut, Universität zu Köln, Zülpicher Straße 77, D-50937 Köln, Germany

P. Thaddeus
Harvard-Smithsonian Center for Astrophysics, Cambridge, Massachusetts 02138
and Division of Engineering and Applied Sciences, Harvard University, Cambridge, Massachusetts 02138

(Received 25 September 2002; accepted 8 November 2002)

Two new carbon chain radicals terminated with a nitrile group, C_4N and C_6N, have been detected in a supersonic molecular beam by Fourier transform microwave spectroscopy. In addition, at least three hyperfine-split rotational transitions of the singly-substituted isotopic species of C_3N have also been observed. Both C_4N and C_6N are linear chains with $^2\Pi$ electronic ground states, and both radicals have resolvable hyperfine structure and lambda-type doubling in their lowest rotational levels. At least four transitions in the lowest-energy fine structure component ($^2\Pi_{1/2}$) were measured between 7 and 22 GHz for both molecules, and at most nine spectroscopic constants were required to reproduce the measured spectra to a few parts in 10^7. Precise sets of rotational, centrifugal distortion, spin-rotation, and hyperfine coupling constants were also determined for the isotopic species of C_3N by combining the centimeter-wave measurements here with previous millimeter-wave data. The ^{13}C hyperfine coupling constants of isotopic C_3N differ from those of the isoelectronic chain C_4H, but are fairly close to those of isovalent C_2H, indicating a nearly pure $^2\Sigma$ electronic ground state for C_3N. Although the strongest lines of C_6N are more than five times less intense than those of C_5N, owing to large differences in the ground state dipole moments, both new chains are more abundant than C_5N. Searches for C_7N have so far been unsuccessful. The absence of lines at the predicted frequencies implies that the product of the dipole moment times the abundance ($\mu \cdot N_a$) is more than 60 times smaller for C_7N than for C_5N, suggesting that the ground state of C_7N may be $^2\Pi$, for which the dipole moment is calculated to be small. © *2003 American Institute of Physics.* [DOI: 10.1063/1.1534104]

I. INTRODUCTION

The violet band of the nitrile radical CN has long been observed in the interstellar gas,[1] and two carbon chains terminated with a nitrile group, C_3N and C_5N, have been detected in interstellar or circumstellar sources with radio telescopes.[2] Owing to their importance as reactive intermediates in chemical and astronomical processes, these three radicals have also been the subject of a number of laboratory investigations over the past 40 years. Each possesses a $^2\Sigma^+$ ground state, and the two longer ones have linear (or nearly linear) heavy atom backbones. Although CN ($\mu = 1.45$ D, Ref. 3) has a substantial permanent electric dipole moment, C_3N (2.78 D, Ref. 4) and C_5N (3.38 D, Ref. 5) are even more polar, with intense rotational lines which have aided their detection in the laboratory and in space.

In contrast, CCN is the only even-membered C_nN radical that has been detected in the gas-phase at any wavelength, even though longer such chains may play important roles in interstellar chemistry and soot formation.[6,7] Like that of CN, the electronic spectrum of CCN was observed more than 25 years[8] before its pure rotational spectrum was measured.[9] Laboratory detection of longer $C_{2n}N$ radicals has proven difficult because these—like CCN—are expected to have $^2\Pi$ electronic ground states and small dipole moments.[10]

A detailed study of the electronic structure of C_3N is also worth undertaking because this radical is isoelectronic with C_4H, a well-studied molecule in which an extremely low-lying $A\,^2\Pi$ electronic state strongly interacts with the $X\,^2\Sigma^+$ ground state.[11] Owing to large zero-order mixing between the two states, the ^{13}C hyperfine coupling constants of C_4H at each substituted position along the chain[12] differ significantly from those of the closely-related chain CCH.[13] Determination of the analogous constants for isotopic C_3N should provide an unambiguous comparison of the electronic structure and chemical bonding for these two isoelectronic radicals.

By means of Fourier transform microwave (FTM) spectroscopy of a supersonic molecular beam, two nitrogen-bearing carbon chain radicals, C_4N and C_6N, have been detected. These have $^2\Pi$ ground states with regular fine structure, and well-resolved lambda-type doubling and hyperfine structure in their lower rotational transitions. All of the chains from C_3N to C_6N have abundances in excess of 10^9 molecules per gas pulse. In spite of their weaker line intensities, C_4N and C_6N are produced more abundantly than C_5N in our molecular beam. A search for the next member in the series, C_7N, has also been undertaken on the basis of high-level *ab initio* calculations; no lines have been detected at the predicted frequencies, suggesting that the ground state may be $^2\Pi$, for which the dipole moment is calculated to be about four times smaller than that for the $^2\Sigma$ state. In addition, we give a detailed account here of the nitrogen-15 and the three carbon-13 isotopic spectra of C_3N.[11] A complete set of hyperfine coupling constants has been determined for each species, which allows detailed comparisons to be made with carbon-13 CCH and C_4H.

II. EXPERIMENT

Rotational lines of the two new radicals here and isotopic C_3N were detected at centimeter wavelengths with a sensitive FTM spectrometer that has been used to detect nearly 100 new carbon chains, ring-chains, and silicon–carbon rings during the past 6 years.[14] The spectrometer and the supersonic molecular beam discharge nozzle have been described in previous publications.[15,16] Briefly, a pulsed supersonic molecular beam of an organic precursor vapor heavily diluted in an inert gas is produced by a commercial solenoid valve. Depending on the precursor gas, a wide variety of reactive molecules are formed by applying a small electrical discharge in the throat of the supersonic nozzle, prior to adiabatic expansion. Free expansion from the nozzle forms in a short distance an approximately Mach 2 supersonic beam with a rotational temperature that drops precipitously to as low as 1 K. As the beam passes through a large high-Q Fabry–Perot cavity, a rotational transition resonant with one of the modes of the cavity is excited coherently by a short pulse of microwave radiation. When the pulse is switched off, the stored microwave energy in the cavity rapidly decays away ($\tau < 10\ \mu s$), and line radiation by the coherently rotating molecules ($\tau \sim 75\ \mu s$) is then detected by a sensitive microwave receiver coupled to the cavity by a short L-shaped antenna passing through one of the Fabry–Perot mirrors. The spectrometer operates from 5 to 43 GHz and is fully-computer controlled to the extent that, in spite of the small spectral coverage of each setting of the Fabry–Perot ($\sim$0.5 MHz), automated scans covering wide frequencies and requiring many hours of integration, can be conducted with little or no oversight. Rotational lines of known molecules are routinely monitored for calibration. Care was also taken to minimize the Earth's magnetic field at the center of the Fabry–Perot cavity using three sets of mutually perpendicular Helmholtz coils; the residual of the Earth's field was about 10–15 mG over the active volume of the spectrometer—sufficient cancellation for most of our measurements, but still large enough to broaden the lowest rotational lines of $CCC^{15}N$ beyond the intrinsic instrumental linewidth of 5 kHz.

Searches for the rotational spectra of C_4N and C_6N were guided by *ab initio* calculations of Pauzat *et al.*[10] The rotational constants for both molecules were estimated by scaling the *ab initio* rotational constants by the ratio of the experimental B value to that calculated at the same level of theory for C_2N, C_3N, and C_5N. Rotational transitions predicted in this way turned out to be quite accurate: to within 0.25% for C_4N and C_6N. For isotopic C_3N, searches for the lowest-frequency hyperfine-split transitions were based on spectroscopic constants derived from a previous millimeter-wave study[11] of the three ^{13}C isotopic species of C_3N and $CCC^{15}N$. In that study, the authors reported effective $b_F(^{13}C)$ values for $^{13}CCCN$ and $C^{13}CCN$, but they were unable to determine the dipole–dipole constant c or the ^{14}N hyperfine coupling constants for either isotopic species—or to observe hfs for either $CC^{13}CN$ or $CCC^{15}N$.

The optimal experimental conditions for the present molecules were found to be similar to those that optimize production of the acetylenic free radicals C_nH: a low-current dc discharge of 1100–1300 V synchronized with a 300–480 μs long gas pulse at a total pressure behind the nozzle of 2.5 kTorr (3.2 atm), and a total gas flow of 25–35 sccm. The strongest lines of C_4N and C_6N were obtained with a mixture of 0.2% HC_3N in Ne, while lines of the ^{13}C isotopic species of C_3N were detected with a mixture of 0.2% HC_3N and 0.7% statistical carbon-13 HCCH (i.e., 25% HCCH, 50% $H^{13}CCH$, and 25% $H^{13}C^{13}CH$) in Ne; 0.2% $CH_3C^{15}N$ in Ne was used to detect the $CCC^{15}N$ isotopic species, and a sample of 0.2% $CH_3{}^{13}CN$ in Ne was used to confirm our tentative detection of $CC^{13}CN$. The statistical mixture of carbon-13 HCCH was produced by the hydrolysis of ^{13}C-enriched Li_2C_2 which was prepared by the NIH Stable Isotope Resource, Los Alamos National Laboratory.

The present identifications are extremely secure: (i) the two new molecules are almost certainly radicals because their rotational transitions are separated in frequency by half-integer quantum numbers, and their lines exhibit the expected Zeeman effect (i.e., a fairly modest broadening owing to the small magnetic g factor of a $^2\Pi_{1/2}$ state) when a permanent magnet is brought near the molecular beam; (ii) the carriers of the observed lines are nitrogen-bearing molecules because the lines disappear when cyanoacetylene is replaced with diacetylene, and because characteristic hfs from the nitrogen nucleus was observed in all of the assigned spectra; (iii) impurities from contaminants in the gas samples, as well as van der Waals complexes with the buffer gas, can also be ruled out, because the lines were produced with acetylene plus cyanogen as the precursor gas, and when Ar replaced Ne as the buffer gas; and (iv) the identifications of C_4N and C_6N are also supported on spectroscopic grounds by the close agreement of B and D with those estimated by scaling from the *ab initio* geometries and the C_nH chains of similar size. In addition, the lambda-doubling constant $p+2q$ in the $^2\Pi_{1/2}$ ladder of C_4N and C_6N can be predicted to within a factor of 2 by scaling from CCN (Ref. 9) on the assumption of free precession. The nitrogen hyperfine constants $a-(b+c)/2$, b,

and d also smoothly decrease in magnitude from CCN to C_6N, as one might expect if the unpaired electron is delocalized along the chain; a similar decrease in the hydrogen hyperfine constant $a-(b+c)/2$ has been observed in the odd-numbered acetylenic chains up to $C_{13}H$.[17]

Under optimized experimental conditions, the strongest rotational lines of C_4N were approximately 15 times less intense than those of C_3N, but were still observed with a signal to noise of approximately 25 after 1 min of integration; the decrement in peak signal strength from C_4N to C_6N was only about a factor of 3. For speed and convenience, all of the C_3N isotopic measurements were made with enriched samples; with the ^{13}C-HCCH sample, line intensities were typically 2–3 times stronger than those of the same lines observed in natural abundance. When the ^{13}C-methylcyanide sample was employed instead, lines of $CC^{13}CN$ were three times more intense than those observed with ^{13}C-acetylene. Sample lines of C_4N, C_6N, and $CCC^{15}N$ are shown in Fig. 1.

Laboratory searches were also undertaken for C_7N using experimental conditions and gas mixtures that optimize the production of either C_5N or C_6N, or both molecules simultaneously. Searches were based on a high-level coupled cluster calculation of Botschwina,[18] and covered frequency ranges that correspond to $\pm 1\%$ of the predicted rotational constants. Two searches, one assuming a $^2\Sigma$ ground state with rotational lines separated in frequency by integer quantum numbers, and one assuming a $^2\Pi$ ground state with rotational lines separated in frequency by half-integer quantum numbers, were performed, but no lines which could be attributed to C_7N were found in either survey. The absence of lines requires the C_7N line intensities to be at least 60 times less than those of C_5N, which is readily observed in our molecular beam with a signal to noise of better than 25 in 1 min of integration.

III. DATA AND ANALYSIS

A. C_4N and C_6N

The lowest rotational transitions of both C_4N and C_6N in the ground $^2\Pi_{1/2}$ fine structure ladder are split into six components by Λ-doubling on the scale of 2–5 MHz and then by hfs from the nitrogen nucleus which is generally smaller by about an order of magnitude. At least four rotational transitions of each radical fall within the frequency range of our spectrometer; those measured are given in Tables I and II, respectively. Rotational transitions from the higher-lying $X\,^2\Pi_{3/2}$ ladder were not observed, because this lies at least several tens of Kelvin above the $X\,^2\Pi_{1/2}$ ladder and is apparently not appreciably populated in the generally rotationally cold molecular beam ($T_{\rm rot}=2-3$ K). An effective Hamiltonian for a molecule in a $^2\Pi$ electronic state[19–21] was fit to the measured transitions. With the fine structure constant A constrained at 40 cm^{-1}, at most nine spectroscopic constants: the rotational constant B, centrifugal distortion D, two lambda-doubling constants $p+2q$ and $(p+2q)_D$, and five hyperfine constants, the diagonal term $a_-=a-(b+c)/2$, the off-diagonal term b, the parity-dependent term d, the electric quadrupole term eQq_0, and the nonaxially symmetric quadrupole term eQq_2 were required to reproduce the 29 mea-

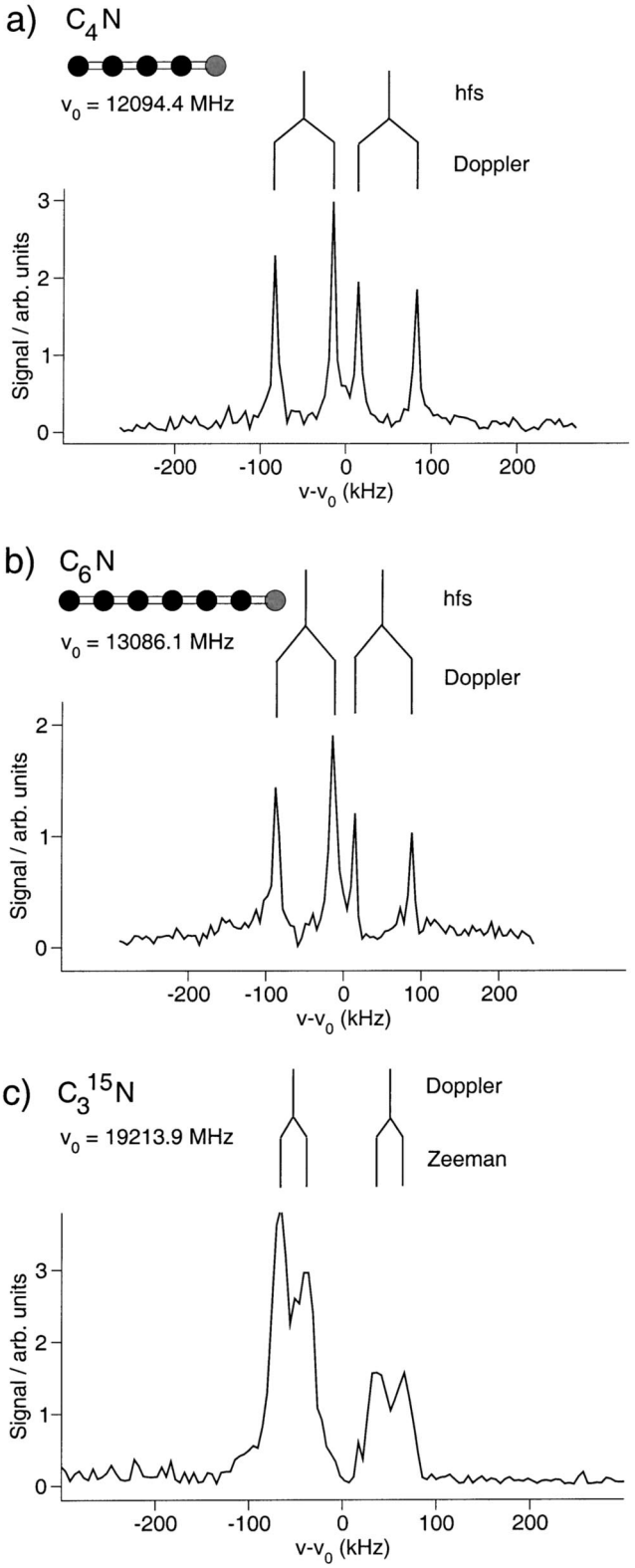

FIG. 1. Sample rotational spectra of (a) C_4N, (b) C_6N, and (c) $CCC^{15}N$. The valence structures indicated at the top of the C_4N and C_6N spectra are only approximate. Owing to large lambda-doubling, only one lambda component is shown here for both C_4N and C_6N. For $CCC^{15}N$, incomplete cancellation of the magnetic field in the center of the Fabry–Perot cavity splits the observed line into two Zeeman components, which are separated in frequency by 20–30 kHz. In each spectrum, the double-peaked line profile is an instrumental artifact: Doppler splitting results from the interaction of the supersonic axial molecular beam with the standing wave of the confocal Fabry–Perot microwave cavity. The integration time for each spectrum was approximately 4 min, i.e., the coaddition of approximately 1500 free induction decays at the 6 Hz repetition rate of the nozzle.

TABLE I. Measured rotational transitions of C_4N in the $X\ ^2\Pi_{1/2}$ state.

Transition		Frequency[a]	e/f	O−C[c]
$J'\rightarrow J$	$F'\rightarrow F$	(MHz)	Λ Comp.[b]	(kHz)
1.5→0.5	1.5→1.5	7234.345	*f*	1
	2.5→1.5	7247.840	*e*	−1
	1.5→0.5	7249.186	*e*	0
	2.5→1.5	7255.402	*f*	−1
	1.5→1.5	7256.628	*e*	−1
	0.5→0.5	7257.124	*e*	0
	0.5→0.5	7261.707	*f*	0
	1.5→0.5	7271.774	*f*	−1
2.5→1.5	2.5→2.5	12 073.322	*f*	−1
	1.5→1.5	12 084.411	*f*	−1
	3.5→2.5	12 085.235	*e*	1
	1.5→0.5	12 086.839	*e*	0
	3.5→2.5	12 091.162	*f*	2
	2.5→2.5	12 094.262	*e*	2
	2.5→1.5	12 094.384	*f*	1
	1.5→0.5	12 094.480	*f*	0
	1.5→1.5	12 094.777	*e*	0
3.5→2.5	4.5→3.5	16 921.368	*e*	−1
	3.5→2.5	16 921.448	*e*	−1
	2.5→1.5	16 922.195	*e*	0
	4.5→3.5	16 926.823	*f*	1
	3.5→2.5	16 928.186	*f*	−1
	2.5→1.5	16 928.220	*f*	−0
4.5→3.5	5.5→4.5	21 757.146	*e*	2
	4.5→3.5	21 757.171	*e*	−1
	3.5→2.5	21 757.636	*e*	−0
	5.5→4.5	21 762.464	*f*	−1
	4.5→3.5	21 763.210	*f*	−1
	3.5→2.5	21 763.220	*f*	2

[a]Estimated experimental uncertainties (1σ) are 2 kHz.
[b]Designation of *e* and *f* levels is based on the assumption that the hyperfine constant *d* is positive.
[c]Calculated frequencies derived from the best fit constants in Table III.

sured lines of C_4N and the 42 of C_6N to better than 2 kHz. If eQq_2 was constrained to zero in the C_4N fit, the rms increases by more than a factor of 5. The spectroscopic constants obtained from the fits are given in Table III.

B. Isotopic species of C_3N

The rotational spectra of the singly-substituted isotopic species of CCCN were analyzed with a standard Hamiltonian for a linear $^2\Sigma$ molecule with two nuclear spins,[22] as done previously for the carbon-13 isotopic species of CCCCH.[11] Owing to the relative magnitude of the spin-rotation and magnetic hyperfine interactions, the coupling scheme

$$\mathbf{J}=\mathbf{N}+\mathbf{S},\quad \mathbf{F}_1=\mathbf{J}+\mathbf{I}(^{13}\mathrm{C}),\mathbf{F}=\mathbf{F}_1+\mathbf{I}(\mathrm{N}) \tag{1}$$

was used to analyze the three carbon-13 species. For $CCC^{15}N$, the coupling scheme simplifies to $\mathbf{J}=\mathbf{N}+\mathbf{S}$, $\mathbf{F}=\mathbf{J}+\mathbf{I}(^{15}\mathrm{N})$. For $^{13}CCCN$, a more natural choice for the coupling scheme would be $\mathbf{F}_1=\mathbf{N}+\mathbf{I}(^{13}\mathrm{C})$, $\mathbf{F}_2=\mathbf{F}_1+\mathbf{S}$, $\mathbf{F}=\mathbf{F}_2+\mathbf{I}(\mathrm{N})$ because the ^{13}C hyperfine interaction is larger than that of spin-rotation.[23] However the fitting program can readily handle large off-diagonal terms in the Hamiltonian matrix which occur when the coupling scheme in Eq. (1) is used, so, for uniformity, this program was used for $^{13}CCCN$ as well. The energy level diagram in Fig. 2 shows schematically the spin-rotation and hyperfine splitting for the lower rotational levels of $^{13}CCCN$, as well as some of the stronger transitions that have been observed.

At least three hyperfine-split rotational transitions were observed for each of the four singly-substituted isotopic species of CCCN. Table IV gives the frequencies of the observed transitions and their assignments. The observed hyperfine components are generally those with the strongest predicted intensities; some of the weaker ones are too faint to detect.

In initial fits to the carbon-13 FTM centimeter-wave data in Table IV, the rotational constant *B*, and the centrifugal distortion constant *D* were constrained to the values previ-

TABLE II. Measured rotational transitions of C_6N in the $X\ ^2\Pi_{1/2}$ state.

Transition		Frequency[a]	e/f	O−C[c]
$J'\rightarrow J$	$F'\rightarrow F$	(MHz)	Λ Comp.[b]	(kHz)
4.5→3.5	5.5→4.5	7851.036	*e*	−1
	4.5→3.5	7851.047	*e*	0
	3.5→2.5	7851.318	*e*	0
	5.5→4.5	7853.245	*f*	−3
	4.5→3.5	7853.677	*f*	0
	3.5→2.5	7853.677	*f*	−4
5.5→4.5	6.5→5.5	9596.072	*e*	2
	5.5→4.5	9596.072	*e*	−2
	4.5→3.5	9596.260	*e*	0
	6.5→5.5	9598.199	*f*	−1
	5.5→4.5	9598.474	*f*	3
	4.5→3.5	9598.474	*f*	2
6.5→5.5	7.5→6.5	11 341.066	*e*	−1
	6.5→5.5	11 341.066	*e*	−2
	5.5→4.5	11 341.203	*e*	0
	7.5→6.5	11 343.149	*f*	−1
	6.5→5.5	11 343.336	*f*	0
	5.5→4.5	11 343.336	*f*	0
7.5→6.5	8.5→7.5	13 086.043	*e*	−1
	7.5→6.5	13 086.043	*e*	0
	6.5→5.5	13 086.146	*e*	0
	8.5→7.5	13 088.099	*f*	1
	7.5→6.5	13 088.233	*f*	0
	6.5→5.5	13 088.233	*f*	2
8.5→7.5	9.5→8.5	14 831.011	*e*	2
	8.5→7.5	14 831.011	*e*	4
	7.5→6.5	14 831.085	*e*	−1
	9.5→8.5	14 833.047	*f*	3
	8.5→7.5	14 833.145	*f*	−1
	7.5→6.5	14 833.145	*f*	2
9.5→8.5	10.5→9.5	16 575.963	*e*	−1
	9.5→8.5	16 575.963	*e*	1
	8.5→7.5	16 576.024	*e*	−1
	10.5→9.5	16 577.985	*f*	−2
	9.5→8.5	16 578.067	*f*	0
	8.5→7.5	16 578.067	*f*	3
10.5→9.5	10.5→9.5	18 320.906	*e*	−4
	11.5→10.5	18 320.916	*e*	3
	9.5→8.5	18 320.973[d]	*e*	···
	11.5→10.5	18 322.929	*f*	1
	9.5→8.5	18 322.986	*f*	−2
	10.5→9.5	18 322.990	*f*	−2

[a]Estimated experimental uncertainties (1σ) are 2 kHz.
[b]Designation of *e* and *f* levels is based on the assumption that the hyperfine constant *d* is positive.
[c]Calculated frequencies derived from the best fit constants in Table III.
[d]Overlapped with interloping line; not included in fit.

TABLE III. Spectroscopic constants of C_4N and C_6N in the $X\ ^2\Pi$ state.

Constant[a]	C_4N	C_6N
A_{eff}	1 200 000[b] (40 cm^{-1})	1 200 000[b] (40 cm^{-1})
B	2422.6963(1)	873.112 24(6)
$D\times10^6$	90(3)	11.5(4)
$p+2q$	4.5525(8)	1.939(3)
$(p+2q)_D\times10^3$	5.23(2)	0.066(10)
$a-(b+c)/2$	15.005(1)	8.7(5)
b	16.2(1)	7.4(10)
d	22.4254(9)	13.23(8)
eQq_0	−4.389(1)	−4.38[b]
eQq_2	5.6(3)	⋯

[a]Units are MHz. The 1σ uncertainties (in parentheses) are in the units of the last significant digits.
[b]Fixed.

ously determined from the millimeter-wave data, and the three nitrogen hyperfine constants (b_F, c, and eQq) were constrained to the values for normal CCCN.[24] The three remaining constants, the spin-rotation constant γ, $b_F(^{13}\text{C})$, and $c(^{13}\text{C})$, were varied to fit the lowest-J transitions, yielding a rms of typically $\leqslant$20 kHz; subsequently, B and the three nitrogen constants were varied as well, giving an rms comparable to the 2–5 kHz measurement uncertainty. For $CCC^{15}N$, the same procedure was used, except initial values for b_F and c were derived by scaling the ^{14}N hyperfine constants for the normal species by the ratio of μ_I/I for the ^{15}N and the ^{14}N nucleus.

After the centimeter-wave transitions were assigned, global fits including the millimeter-wave data[11] were done. The centimeter-wave lines were assigned a frequency uncertainty of 2–5 kHz, and the millimeter-wave lines uncertainties of between 15 kHz and 150 kHz, with 25 kHz for most. Each hyperfine line was thus given a weight of about 100 relative to each of the 5–7 millimeter-wave lines in the range of $N=11-29$. The final hyperfine parameters derived from the global fits are nearly identical to those calculated from the initial fits, and the global rms are comparable to those obtained from the millimeter-wave data alone. Table V lists the spectroscopic parameters determined from the global fit for each singly substituted isotopic species of CCCN—the best summary of all the data at hand. For comparison, the spectroscopic constants of normal CCCN from Ref. 24 are also given.

IV. RESULTS AND DISCUSSION

Lines of C_4N and C_6N are readily observed in our supersonic molecular beam, even though both radicals are cal-

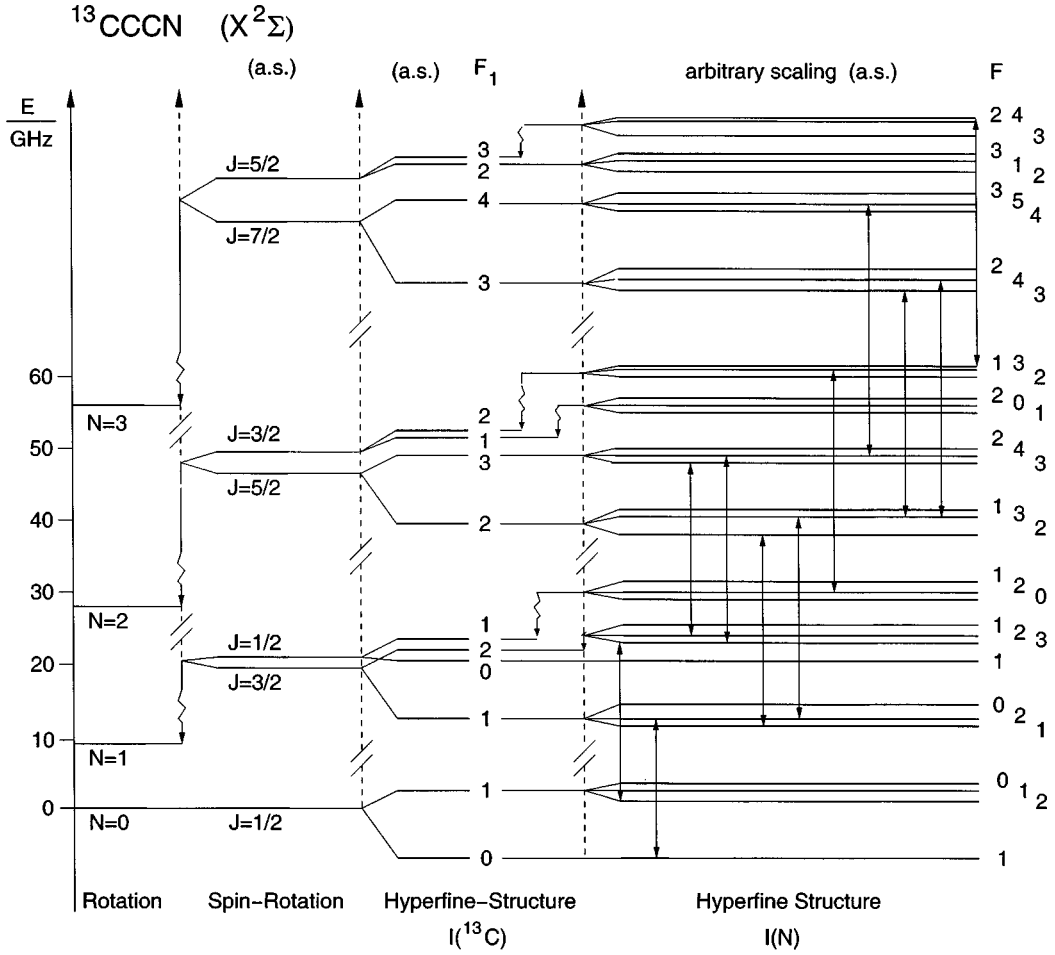

FIG. 2. Energy level diagram showing the effects of spin-rotation and ^{13}C and H hyperfine interactions on the lower rotational levels of $^{13}CCCN$. Arrows indicate measured transitions.

TABLE IV. Measured rotational transitions of the carbon-13 isotopic species of CCCN and CCC^{15}N in the $X\,^2\Sigma^+$ state.

Molecule	Frequency[a] (MHz)	O−C[b] (kHz)	Transition $N'\rightarrow N$	$J'\rightarrow J$	$F_1'\rightarrow F_1$	$F'\rightarrow F$
^{13}CCCN	9528.817	1	1→0	3/2→1/2	2→1	3→2
	9542.475	−3			1→0	2→1
	19 073.604	−2	2→1	5/2→3/2	3→2	3→2
	19 073.886	−1				4→3
	19 084.532	−3			2→1	2→1
	19 084.612	3				3→2
	19 085.382	0		3/2→1/2	2→1	3→2
	28 617.158	2	3→2	7/2→5/2	4→3	5→4
	28 626.762	1			3→2	3→3
	28 626.796	4				4→3
	28 627.817	−3		5/2→3/2	3→2	4→3
C^{13}CCN	9829.369	−1	1→0	3/2→1/2	2→1	2→1
	9830.396	1				3→2
	9839.603	−1			1→0	1→1
	9840.701	−2				2→1
	19 672.508	6	2→1	5/2→3/2	3→2	3→2
	19 672.780	−5				4→3
	19 681.164	−7			2→1	3→2
	19 681.175	3				2→1
	19 684.220	1		3/2→1/2	2→1	1→1
	19 684.755	2				3→2
	29 521.725	3	3→2	7/2→5/2	3→2	4→3
	29 521.758	1				3→2
	29 626.764	−4		5/2→3/2	3→2	4→3
CC^{13}CN	9847.713	−3	1→0	3/2→1/2	2→1	2→1
	9848.755	2				3→2
	9853.055	5			1→0	1→1
	9853.282	8				2→1
	9873.604	2		1/2→1/2	1→1	2→2
	19 706.620	3	2→1	5/2→3/2	3→2	3→2
	19 706.889	2				4→3
	19 706.914	3				2→1
	19 709.044	−7			2→1	2→1
	19 709.080	5				3→2
	19 723.673	3		3/2→1/2	2→1	3→2
	19 726.516	−3			1→0	2→1
	29 564.843	0	3→2	7/2→5/2	4→3	4→3
	29 564.907	−3				3→2
	29 564.970	2				5→4
	29 566.119	−3			3→2	3→2
	29 566.174	5				4→3
	29 568.747	−6	3→2	7/2→5/2	3→2	2→2
	29 580.140	−2		5/2→3/2	3→2	3→3
	29 581.389	−3			2→1	2→2
	29 582.300	−8			3→2	3→2
	29 582.480	3				2→1
	29 582.569	1				4→3
	29 583.673	0			2→1	2→1
	29 583.913	5				3→2
	29 584.491	1				1→1
	39 422.912	−5	4→3	9/2→7/2	5→4	5→4
	39 422.990	1				6→5
	39 440.879	−1		7/2→5/2	4→3	4→3
	39 440.986	0				5→4
	39 441.702	−2			3→2	3→2
	39 441.485	6				4→3
CCC^{15}N	9593.486	−4	1→0	3/2→1/2		2→1
	19 195.842	0	2→1	5/2→3/2		3→2
	19 195.863	1				2→1
	19 213.911	4		3/2→1/2		2→1
	19 243.521	0				1→1
	28 798.215	1	3→2	7/2→5/2		4→3
	28 798.215	−1				3→2
	28 816.243	−2		5/2→3/2		2→1
	28 816.350	−3				3→2
	38 400.553	2	4→3	9/2→7/2		5→4
	38 400.553	4				4→3

[a]Estimated experimental uncertainties (1σ) are 2 kHz, except for the CC^{13}CN transitions whose uncertainties are 5 kHz.

[b]Calculated frequencies derived from the best fit constants in Table V.

culated *ab initio* to possess rather small dipole moments: 0.14 D for C_4N and 0.31 D for C_6N.[10] In FTM spectroscopy, line strengths are proportional to the first power of the dipole moment μ, not μ^2, as in classical absorption spectroscopy; rotational lines of small μ molecules are therefore relatively much more intense in FT spectroscopy than in conventional spectroscopy. Bauder and co-workers, for example, have detected a number of deuterated hydrocarbons[25] using the present technique; many with dipole moments in the range of 10^{-1}–10^{-3} D.

Relative abundances (Fig. 3) of the nitrogen-bearing carbon chain radicals here to one another and to C_3N and C_5N were determined from intensity measurements on lines as close in frequency as possible to minimize variations in instrumental gain. These were converted to absolute abundances by comparing line intensities with those of the rare isotopic species of OCS in a supersonic beam of 1% OCS in Ar in the absence of a discharge, taking into account differences in the rotational partition functions and dipole moments. As Fig. 3 shows, the two new chains here are more than a factor of 2 more abundant than C_5N.

Our failure to detect C_7N may indicate a $^2\Pi$ ground state for this molecule. Botschwina concluded on the basis of RCCSD(T)/cc-pVTZ calculations[18] that the ground state of C_7N is $^2\Pi$ ($\mu=0.96$ D), but that a $^2\Sigma^+$ state ($\mu=3.86$ D) is very close in energy, lying only 250 cm^{-1} above ground at the highest level of theory. If we assume the same abundance decrement from C_5N to C_7N as from C_3N to C_5N (a factor of 17) and a $^2\Pi$ ground state, the C_7N lines would be 180 less intense than those of C_5N, i.e., three times below our present upper limit. If the ground state is $^2\Sigma^+$ instead, the expected decrease in line intensity is only a factor of 45. In either case, significant rovibronic interaction may occur between these two low-lying electronic states, a factor which could hinder spectral analysis and assignment regardless of the symmetry of the ground state. Detection of C_7N may still be possible; with further improvements in instrumentation and production efficiency a factor of 5 or more in sensitivity may be within reach.

The formation of carbon chain radicals in our molecular beam is apparently different for chains with odd and even numbers of carbon atoms. Although the abundance data for C_nN is much less complete than for C_nH, it is worth noting that the plot in Fig. 3 is similar to that previously derived for the acetylenic radicals (see Fig. 2 of Ref. 17), implying similar, if not common, formation mechanisms in our discharge. Most of the $C_{2n+1}H$ and $C_{2n}N$ chains are more abundant than the corresponding $C_{2n}H$ and $C_{2n+1}N$ chains. If nonpolar carbon chains C_{2n+1} are more abundant than even-numbered chains C_{2n}, for example, subsequent reactions involving the radicals C_2H or CN (produced directly via cleavage of the central C–C bond of either HC_4H or HC_3N) may produce the odd–even alternation that is observed. Evidence to support this formation mechanism is the mass distribution of a diacetylene discharge which exhibits an even–odd alternation in abundance for chains beyond C_9, with the odd chains being more abundant.[26] Additional isotopic spectroscopy using ^{13}C-enriched samples of cyanogen, cyanoacetylene, methylcyanide, etc., may allow the distribution of carbon in our

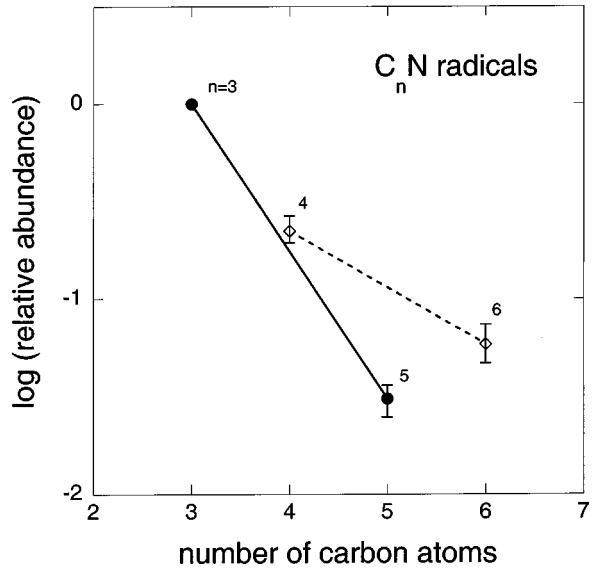

FIG. 3. Relative abundances of the C_nN radicals per gas pulse in the supersonic molecular beam as a function of chain length.

discharge source to be determined, providing clues to the chemical processes at work.

Low-lying isomers of C_4N and C_6N may be amenable to laboratory detection with present techniques. Ding *et al.*[27] recently calculated the potential energy surface of C_4N, and concluded that 13 isomers, some with unusual cyclic, branched, and caged structures, probably exist. The isomer of the most immediate laboratory interest is the ring-chain analog to c-C_5H, with the CCH group replaced by a nitrile group. This isomer is predicted to have considerable kinetic stability towards isomerization and dissociation, and is calculated to lie only 2.8 kcal/mol above the linear chain. Because it is also predicted to possess a substantial dipole moment ($\mu = 0.63$ D), and because c-C_5H has already been detected with the same discharge source,[28] detection of c-C_4N may succeed with dedicated searches. Other low-lying polar isomers of C_4N such as CCCNC (23.4 kcal/mol; 1.38 D) may also be within reach.

The electronic spectra of C_4N and C_6N as far as we can tell are completely unknown. Both radicals probably possess strong $^2\Pi - X\,^2\Pi$ electronic transitions at visible or near-infrared wavelengths, like the shorter chain CCN (Ref. 9) and most of the acetylenic chains C_nH up to $C_{10}H$. Many of these have now been studied by sensitive laser techniques (see e.g., Ref. 29), including LIF, cavity ring-down laser absorption spectroscopy (CRLAS), and most recently, resonant two-color, two-photon ionization spectroscopy (R2C2PI) combined with time-of-flight mass detection. All of the species up to C_6N have abundances near the throat of our nozzle of $>10^9$ molecules per pulse—an adequate number density for all three techniques—but the best choice would appear to be R2C2PI because the optical spectrum of linear C_3H is significantly broadened owing to rapid internal conversion,[30] and because REMPI is more sensitive than CRLAS and is mass selective as well.

With the ^{13}C hyperfine constants given in Table V, it is possible to make systematic comparisons between the electronic structure and chemical bonding of C_3N, isoelectronic C_4H, and isovalent CCH. Such comparisons are appropriate because all three chains are σ-bonded radicals with $^2\Sigma$ ground states, and because the hyperfine constants are proportional to important expectation values of the valence electron, providing highly specific probes of the molecular wave function. Carbon-13 is particularly useful because it probes the wave function at all the substituted positions along the carbon chain.

There are only two nonzero hyperfine parameters for a $^2\Sigma$ state: the Fermi-contact term b_F and the dipole–dipole term c. The Fermi-contact term sheds light on the location of the unpaired electron along the carbon chain backbone, because only s electrons have nonzero amplitude at $r = 0$, and the unpaired electron is expected to have significant s character for the three σ-bonded radicals here. The dipole–dipole term c also provides information on the orbital occupancies of the unpaired electron, because it is a function of both an angular average and the radial expectation value of $1/r^3$.

Figure 4 shows the magnitude of the two hyperfine con-

TABLE V. Spectroscopic constants of the CCCN isotopic species.

Constant[a]	CCCN[b]	^{13}CCCN	C^{13}CCN	CC^{13}CN	CCC^{15}N
B	4947.6207(11)	4771.2195(2)	4920.7095(2)	4929.0640(2)	4801.2267(1)
$D\times10^3$	0.7535(16)	0.6993(2)	0.7453(4)	−0.7497(3)	0.7064(1)
γ	−18.744(6)	−17.963(5)	−18.574(5)	−18.648(3)	−18.208(1)
$\gamma_D\times10^3$	−0.006(11)	⋯	⋯	⋯	⋯
$b_F(^{13}C)$	⋯	973(2)	188.6(2)	23.55(2)	⋯
$c(^{13}C)$	⋯	139.5(3)	52.9(1)	2.17(3)	⋯
$b_F(^{14}N)$	−1.20(3)	−1.26(6)	−1.234(6)	−1.182(8)	⋯
$c(^{14}N)$	2.84(9)	3.4(1)	2.82(3)	2.88(2)	⋯
eQq_0	−4.32(10)	−4.48(4)	−4.331(9)	−4.323(8)	⋯
$b_F(^{15}N)$	⋯	⋯	⋯	⋯	1.883(9)
$c(^{15}N)$	⋯	⋯	⋯	⋯	−4.30(3)
σ_N[c]	⋯	1.19	1.16	0.77	0.97

[a]Units are MHz. The 1σ uncertainties (in parentheses) are in the units of the last significant digits. The spectroscopic constants were derived from the hyperfine-split centimeter-wave transitions in Table IV and the millimeter-wave transitions in Ref. 11.
[b]Reference 24.
[c]Normalized standard deviation of the fit.

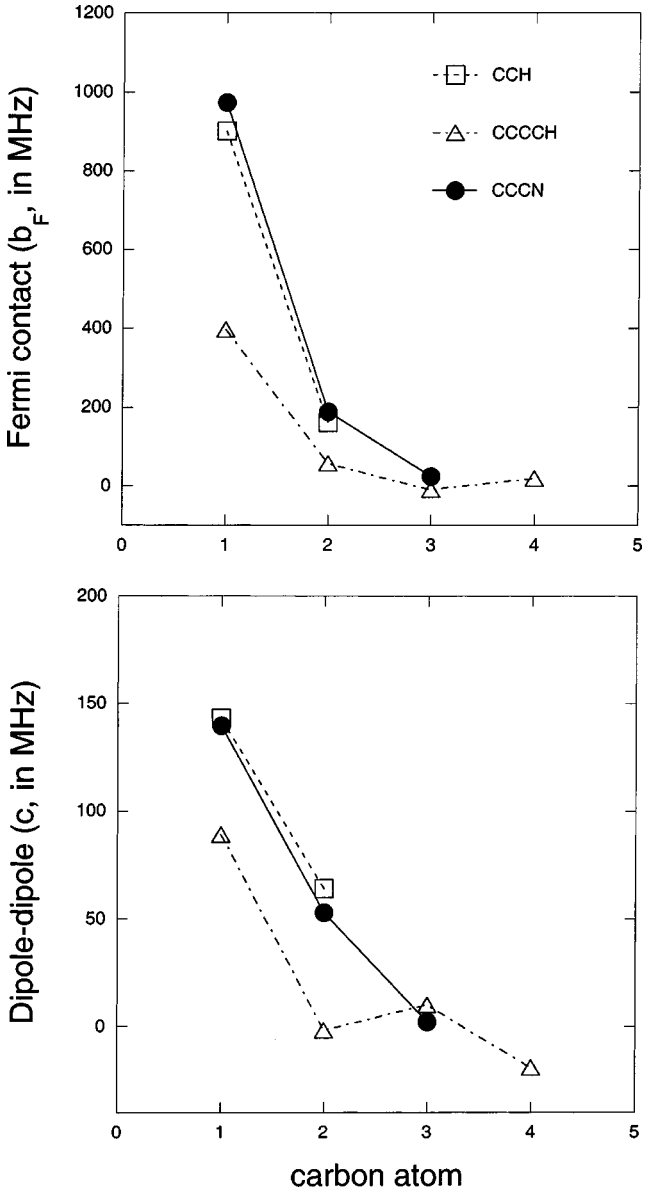

FIG. 4. Comparison of the ^{13}C hyperfine constants for C_2H, C_4H, and C_3N at different substituted positions along the chain; the positions are numbered with respect to the terminal carbon atom. The C_2H data are from Ref. 13 and the C_4H data are from Ref. 12.

stants at different positions along the carbon chain for the three radicals. Although $b_F(^{13}C)$ and $c(^{13}C)$ are nearly the same for ^{13}CCH and $^{13}CCCN$ and for $C^{13}CH$ and $C^{13}CCN$, the same two constants are each smaller by about a factor of 2 or more at the same substituted positions of CCCCH. The reason for these differences may be the large zero-order mixing between the low-lying $^2\Pi$ state and the $X\,^2\Sigma^+$ ground state of C_4H: the $^2\Pi - X\,^2\Sigma$ energy separation is calculated to be 3600 cm^{-1} for CCH,[31] 2400 ± 50 cm^{-1} for C_3N, but only 100 ± 50 cm^{-1} for C_4H.[11] Owing to strong vibronic coupling between these states, the $^2\Sigma$ ground state of C_4H probably possesses significant $^2\Pi$ character, unlike the ground states of CCH or C_3N, which are nearly pure $^2\Sigma$.

With simple atomic orbitals[32] it is possible to estimate crudely the fractional $2s$ and $2p$ character in the 2σ molecular orbital of C_3N, on the assumption the unpaired electron is localized on either of the two carbon atoms furthest from the nitrogen. Within a few percent, this calculation yields the same unpaired electron spin density on the terminal carbon atom (74%) and adjacent carbon atom (26%) for C_3N as that previously derived for CCH,[13] and little contribution from the $p\pi$ electronic configuration. In contrast, the relative amount of $p\pi$ character is estimated by the same calculation[11] to be about 28% for C_4H, a result in good agreement with that of Hoshina *et al.*,[33] who concluded on the basis of LIF measurements that the admixture is about 40%.

The measurements reported here should serve as a guide for future astronomical observations of C_4N, C_6N, and the isotopic species of C_3N. The spectroscopic constants provided in Tables III and V allow the astronomically most interesting radio lines of these to be predicted to an uncertainty of 0.30 $km\,s^{-1}$ or better up to 50 GHz. Astronomical detection of the carbon-13 species of C_3N in the cold molecular cloud TMC-1 is also likely, because they have already been detected by Cernicharo *et al.*[34] in the circumstellar shell of the evolved carbon star IRC+10216.

ACKNOWLEDGMENTS

We thank V. D. Gordon for assistance with early experiments, J. Dudek for synthesis of precursor gases, E. S. Palmer for assistance with microwave electronics, E. W. Gottlieb for assistance with spectral analysis, and M. E. Sanz and C. A. Gottlieb for helpful discussions. The work at Cambridge is supported by NASA Grant No. NAG5-9379 and NSF Grant No. AST-9820722.

[1] A. McKellar, Publ. Astron. Soc. Pac. **52**, 307 (1940).
[2] M. Guélin, N. Neningner, and J. Cernicharo, Astron. Astrophys. **335**, L1 (1998), and references therein.
[3] R. Thomson and F. W. Dalby, Can. J. Phys. **46**, 2815 (1968).
[4] P. Botschwina, M. Horn, J. Fluegge, and S. Seeger, J. Chem. Soc., Faraday Trans. **89**, 2219 (1993).
[5] P. Botschwina, Chem. Phys. Lett. **259**, 627 (1996).
[6] S. D. Doty and C. M. Leung, Astrophys. J. **502**, 898 (1998).
[7] T. I. Hasegawa and E. Herbst, Mon. Not. R. Astron. Soc. **263**, 589 (1993).
[8] A. J. Merer and D. N. Travis, Can. J. Phys. **43**, 1795 (1965).
[9] Y. Ohshima and Y. Endo, J. Mol. Spectrosc. **172**, 225 (1995).
[10] F. Pauzat, Y. Ellinger, and A. D. McLean, Astrophys. J. Lett. **369**, L13 (1991).
[11] M. C. McCarthy, C. A. Gottlieb, P. Thaddeus, M. Horn, and P. Botschwina, J. Chem. Phys. **103**, 7820 (1995).
[12] W. Chen, S. E. Novick, M. C. McCarthy, C. A. Gottlieb, and P. Thaddeus, J. Chem. Phys. **103**, 7828 (1995).
[13] M. C. McCarthy, C. A. Gottlieb, and P. Thaddeus, J. Mol. Spectrosc. **173**, 303 (1995).
[14] P. Thaddeus and M. C. McCarthy, Spectrochim. Acta, Part A **57A**, 757 (2001).
[15] M. C. McCarthy, M. J. Travers, A. Kovács, C. A. Gottlieb, and P. Thaddeus, Astrophys. J., Suppl. Ser. **113**, 105 (1997).
[16] M. C. McCarthy, W. Chen, M. J. Travers, and P. Thaddeus, Astrophys. J., Suppl. Ser. **129**, 611 (2000).
[17] C. A. Gottlieb, M. C. McCarthy, M. J. Travers, J.-U. Grabow, and P. Thaddeus, J. Chem. Phys. **109**, 5433 (1998).
[18] P. Botschwina, M. Horn, K. Markey, and R. Oswald, Mol. Phys. **92**, 381 (1997).
[19] J. M. Brown, M. Kaise, C. M. L. Kerr, and D. J. Milton, Mol. Phys. **36**, 553 (1978).
[20] J. M. Brown, E. A. Colbourn, J. K. G. Watson, and F. D. Wayne, J. Mol. Spectrosc. **74**, 294 (1979).
[21] J. M. Brown and J. E. Schubert, J. Mol. Spectrosc. **95**, 194 (1982).
[22] R. A. Frosch and H. M. Foley, Phys. Rev. **88**, 1337 (1952).

[23] C. H. Townes and A. L. Schawlow, *Microwave Spectroscopy* (Dover, New York, 1975).
[24] C. A. Gottlieb, E. W. Gottlieb, P. Thaddeus, and H. Kawamura, Astrophys. J. **275**, 916 (1983).
[25] J. Pliva, A. Valentin, L. Henry, F. Muller, and A. Bauder, J. Mol. Spectrosc. **168**, 442 (1994).
[26] T. Pino, H. Ding, F. Güthe, and J. P. Maier, J. Chem. Phys. **114**, 2208 (2001).
[27] Y. Ding, J. Liu, X. Huang, Z. Li, and C. Sun, J. Chem. Phys. **114**, 5170 (2001).
[28] A. J. Apponi, M. E. Sanz, C. A. Gottlieb, M. C. McCarthy, and P. Thaddeus, Astrophys. J. Lett. **547**, L65 (2001).
[29] H. Linnartz, T. Motylewski, and J. P. Maier, J. Chem. Phys. **109**, 3819 (1998).
[30] H. Ding, T. Pino, F. Güthe, and J. P. Maier, J. Chem. Phys. **115**, 6913 (2001).
[31] M. Perić, B. Engels, and S. D. Peyerimhoff, J. Mol. Spectrosc. **150**, 56 (1991); **150**, 70 (1991).
[32] T. C. Steimle, D. R. Woodward, and J. M. Brown, J. Chem. Phys. **85**, 1276 (1986).
[33] K. Hoshina, H. Kohguchi, Y. Ohshima, and Y. Endo, J. Chem. Phys. **108**, 3465 (1998).
[34] J. Cernicharo, M. Guélin, and C. Kahane, Astron. Astrophys., Suppl. Ser. **142**, 181 (2000).